Clays and Clay Minerals, Vol. 35, No. 5, 373–378, 1987.

INTERVALENCE ELECTRON TRANSFER AND MAGNETIC EXCHANGE IN REDUCED NONTRONITE

PAUL R. LEAR AND JOSEPH W. STUCKI

Department of Agronomy, University of Illinois
Urbana, Illinois 61801

Abstract—The effects of chemical reduction of structural Fe^{3+} in nontronite SWa-1 (ferruginous smectite) on intervalence electron transfer (IT) and magnetic exchange were investigated. Visible absorption spectra in the region 800–400 nm of a chemical reduction series of the SWa-1 nontronite revealed an IT band near 730 nm (13,700 cm^{-1}). Both the intensity and position of this band were affected by the extent of Fe reduction. The intensity increased until the Fe^{2+} content approached 40% of the total Fe, then decreased slightly with more Fe^{2+}. The position of the band also shifted to lower energy as the extent of reduction increased.

Variable-temperature magnetic susceptibility measurements showed that the magnetic exchange in unaltered nontronite is frustrated antiferromagnetic, but ferromagnetic in reduced samples. Magnetic ordering temperatures are in the range 10–50 K, depending on the extent of reduction. The ferromagnetic component in the magnetization curve increased with increasing Fe^{2+} in the crystal structure. The positive paramagnetic interaction likely is due to electron charge transfer from Fe^{2+} to Fe^{3+} through such structural linkages as Fe^{2+}–O–Fe^{3+} (perhaps following a double exchange mechanism), which is consistent with the visible absorption spectra.

Key Words—Intervalence electron transfer, Iron, Magnetic susceptibility, Nontronite, Reduction, UV-visible spectroscopy.

INTRODUCTION

As reviewed by Stucki (1987), the oxidation state of Fe in smectites affects many important clay properties, but the molecular reactions and mechanisms governing these relationships are poorly understood. To understand better the specific processes that occur, the present study was undertaken to examine the changes in optical (electronic) and magnetic properties of nontronite that accompany chemical reduction of structural Fe^{3+}. The visible spectra (800–400 nm) of both unaltered and reduced nontronite samples were obtained to identify the intervalence electron transfer (IT) transitions and to determine the effect of Fe^{2+} content on the intensity of the IT transitions. Magnetic susceptibility and magnetization measurements were used to assess the magnetic ordering and exchange interactions.

BACKGROUND

Intervalence electron transfer

In any mixed-valence compound of the type $A^{3+}B^{2+}$, the potential exists for an electron in the B site to transfer to the A site, creating $A^{2+}B^{3+}$. Mineralogical examples of mixed-valence compounds include magnetite, ilvaite, and vivianite. Such intervalence electron transfer can be used to enhance understanding of the properties of mixed-valence minerals, whether naturally occurring or chemically produced.

IT transitions in minerals are observed as charge-transfer bands in the optical spectra of minerals containing Fe^{2+} and Fe^{3+} in their crystal structures (Hush, 1967). The reduction of structural Fe^{3+} in nontronite results in a color change from yellow to green or blue-green. This green or blue-green color has been identified as a charge-transfer transition and attributed to the presence of Fe^{2+} and Fe^{3+} in the mineral structure (Anderson and Stucki, 1979).

IT transitions occur via vibronic coupling of two states in a mixed-valence system (Schatz, 1980). Vibronic coupling may be understood as the overlap of the vibrational potential energy wells of two symmetrical states, i.e., ($Fe^{3+}Fe^{2+}$) and ($Fe^{2+}Fe^{3+}$), and is illustrated by the vibrational potential energy diagram presented in Figure 1 for electron transfer in one of the normal modes (i.e., an internal molecular coordinate along which an independent vibration of the molecule occurs) of the system. The particular normal mode of the potential energy wells shown is intended to represent the symmetrical breathing mode involving Fe–O at a given Fe center. The potential energy wells for the two states are displaced from one another because the Fe^{2+}–O equilibrium distance differs from the Fe^{3+}–O distance. By virtue of vibronic coupling, the electron transfer between Fe centers occurs through a vibrationally excited state (B*) of the molecule rather than through an electronically excited state, and the electronic ground state for ($Fe^{3+}Fe^{2+}$) is the same as for ($Fe^{2+}Fe^{3+}$). The amount of optical excitation required for the transition ($E_{op} = E_B^* - E_A$) depends on the equilibrium displacement, or difference in the position, of the two potential energy curves. The difference is

referred to as the vibronic (or electron-phonon) coupling parameter and is denoted by λ. The point of intersection (B) between the two curves defines the classical energy of activation required for thermal electron transfer ($E_{th} = E_B - E_A$). For a symmetrical mixed-valence system, E_{op} exceeds E_{th} by a factor of 4 (Hush, 1967).

Magnetic ordering

Magnetic ordering is the directional alignment of atomic magnetic moments due to interactions between atomic centers. In materials which order magnetically, spontaneous ordering occurs only if the sample is below some critical temperature (which varies widely among minerals) such that the magnetic interactions overcome random fluctuations. In phyllosilicates, magnetic ordering is due to the presence of paramagnetic ions in the crystal structure, mainly high-spin Fe^{3+} and Fe^{2+} which have atomic magnetic moments due to five and four unpaired electrons, respectively. In iron-rich minerals such as nontronite, the type of exchange coupling between magnetic cations on adjacent sites determines whether the moments of neighboring cations are aligned parallel (↑↑) or antiparallel (↑↓). The method of exchange via an intervening anion (i.e., a shared O^{2-}) is called superexchange (Kramers, 1934; Anderson, 1950, 1959). In oxides and clay minerals, the Fe^{2+}–O–Fe^{2+} exchange interactions are often ferromagnetic with the atomic moments aligned parallel, and Fe^{3+}–O–Fe^{3+} exchange interactions are generally antiferromagnetic, with the moments aligned antiparallel (Goodenough, 1963; Ballet and Coey, 1982). For mixed-valent Fe^{2+}–O–Fe^{3+} pairs, the magnetic coupling is ferromagnetic and may be due to a charge-transfer process called double exchange (Zener, 1951).

MATERIALS AND METHODS

Materials

The nontronite used in this experiment was the <2-μm fraction of ferruginous smectite SWa-1 (Source Clay Minerals Repository of The Clay Minerals Society) from Grant County, Washington. It has a total Fe content of 20.08% (3.595 mmole/g) and a structural formula according to Goodman *et al.* (1976), of:

$$Na_{0.78}(Si_{7.30}Al_{0.70})(Al_{1.06}Fe_{2.73}Mg_{0.26})O_{20}(OH)_4.$$

No Fe was assigned to tetrahedral sites because, even though Mössbauer work by Goodman *et al.* (1976) reported small amounts in nontronites SWa-1 (6% of total Fe) and Garfield (9% of total Fe), a more recent study by Bonnin *et al.* (1985), employing a variety of spectroscopic techniques, cast doubt on the presence of tetrahedral Fe in these nontronites. Further, room-temperature Mössbauer spectra of sample SWa-1 (Lear and Stucki, unpublished), in which the c* axis of the sample was oriented at 54.7° relative to the γ-ray, required only two octahedral Fe^{3+} doublets to obtain a statistically acceptable fit ($\chi^2 = 0.92$ with 3 million counts per channel). The clay was Na^+-saturated, dialyzed, and freeze-dried before use.

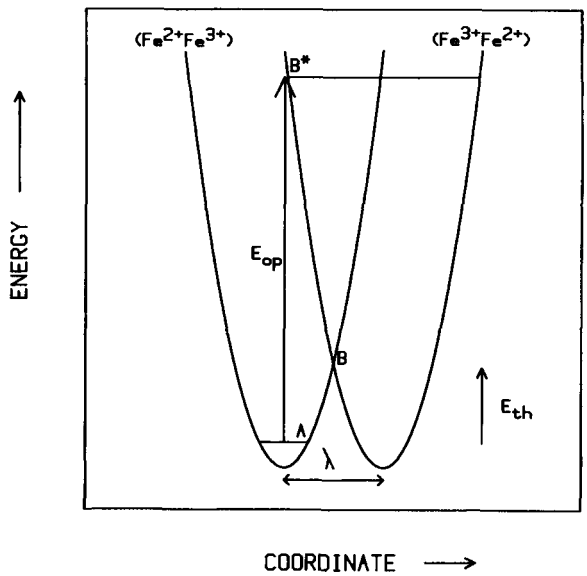

Figure 1. Vibrational potential energy vs. configurational coordinate for electron transfer via vibronic coupling between two symmetrical states of a single oscillator. A, initial state; B*, vibrationally excited state; B, thermally excited state; λ, vibronic coupling parameter; E_{op}, optical transition energy; E_{th}, thermal transition energy. Energy of initial state (left-hand well) is same as final (right-hand well) state (from Hush, 1967).

Methods

Suspensions of sample SWa-1 in a citrate-bicarbonate (C-B) buffer solution were chemically reduced with sodium dithionite ($Na_2S_2O_4$) salt as described by Lear and Stucki (1985). Ferrous iron was determined as described by Stucki (1981); total Fe was determined by atomic absorption.

All visible spectra were measured at room temperature using a Beckman model 5230 UV-visible spectrophotometer equipped with a scattered transmission accessory. A peristaltic pump circulated the clay suspension (2.2 mg of clay/ml) through a flow cell to keep the colloids suspended. The scattered transmission accessory virtually eliminated possible light-scattering differences that were due to variations in particle size among samples. Magnetic susceptibility and magnetization measurements were obtained using a SQUID (superconducting quantum interfering device) magnetometer from SHE Industries for powders of both the reduced and nonreduced nontronite samples.

RESULTS AND DISCUSSION

Stucki *et al.* (1984) recently reported that treatment with C-B solution removes significant amounts of Al

https://doi.org/10.1346/CCMN.1987.0350507 Published online by Cambridge University Press

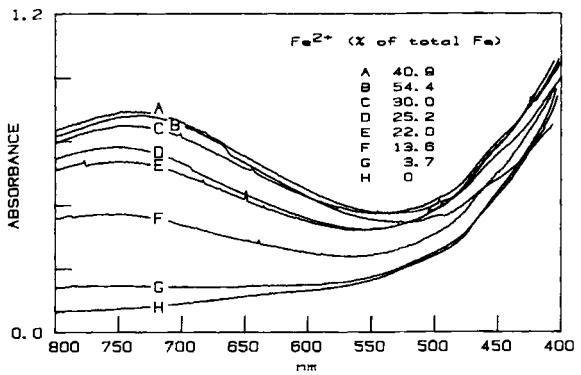

Figure 2. Visible absorption spectra for reduced and unaltered suspensions of sample SWa-1 (2.2 mg clay/ml) in the region 800–400 nm. Inset reports Fe^{2+} content of samples as percentage of total Fe.

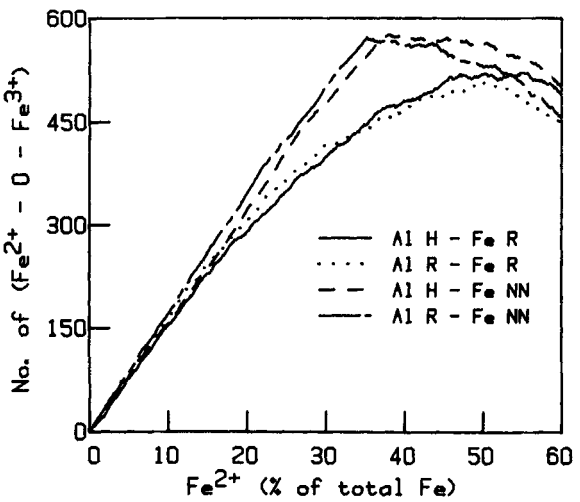

Figure 3. Predicted relationship between number of Fe^{2+}–O–Fe^{3+} linkages and Fe^{2+} content based on computer simulation. Distribution patterns for diamagnetic ions (represented by Al) used were homogeneous (H) and random (R); distribution patterns for Fe^{2+} were random (R) and nearest-neighbor restricted (NN).

and lesser amounts of Fe and Si from clay structures. They suggested, therefore, that some properties of samples reduced with dithionite in C-B could be artifacts of dissolution rather than consequences of Fe reduction. In the present study, the effect of this treatment on optical spectra and magnetic susceptibility was determined by comparing an unaltered sample with a C-B treated sample. No difference was observed in the visible spectrum, and the magnetic susceptibility, although shifted slightly in magnitude, exhibited the same type of exchange interaction in both samples (A and B, Figure 5). Observed differences between unaltered and reduced nontronite, therefore, were attributed to the effect of Fe oxidation state.

Intervalence electron transfer

The IT transition in reduced sample SWa-1 was noted as a broad band centered near 730 nm (13,700 cm^{-1}), which increased in intensity as the Fe^{2+} content increased, then decreased slightly as Fe^{2+} exceeded 40% of the total Fe (B, Figure 2). The center of the band also shifted to lower wavelength as the extent of reduction increased. This band is actually a composite of many individual transitions of Gaussian lineshape, in which the distribution of these transitions determines the position and the profile of the band. The change in position of the maximum as the degree of reduction increased suggests that the distribution of individual IT transitions shifts toward higher energy as more Fe^{2+} is introduced into the mineral structure (Table 1). This shift is especially noticeable if the Fe^{2+} content exceeds 25% of the total Fe (compare C and D, Figure 2).

Table 1. Intensity and position of intervalence electron transfer band for reduced and unaltered SWa-1 samples.

Sample	Fe^{2+} (% of total Fe)	Position (nm)	Intensity (a.u.)[1]
A	40.9	736	0.835
B	54.4	727	0.816
C	29.1	739	0.778
D	25.2	746	0.700
E	22.0	750	0.643
F	13.7	750	0.451
G	3.7	[2]	0.182
H	0	[2]	0.096

[1] a.u. = absorbance units (arbitrary).
[2] No discernible maximum. Intensity listed was determined at 750 nm.

The intensity of the IT band increased directly with Fe^{2+} content (experimental points in Figure 4; Table 1) until about Fe^{2+} = 40% of the total Fe. At this Fe^{2+} content, the intensity decreased slightly (cf. spectra A (40.9% Fe^{2+}) and B (54.4% Fe^{2+}) in Figure 2), thereby suggesting that the absorbance of the IT band is a direct reflection of the number of Fe^{2+}–O–Fe^{3+} entities, which reach a theoretical maximum at Fe^{2+} = 50% of the total Fe. Substantial conversion of Fe^{2+}–O–Fe^{3+} to Fe^{2+}–O–Fe^{2+} at Fe^{2+} contents <50% of the total Fe would produce a non-linear intensity response, because the Fe^{2+}–O–Fe^{2+} groups do not contribute to the IT process. The formation of Fe^{2+}–O–Fe^{2+} in the structure is governed by the probability of Fe^{2+} in adjacent sites, which in turn depends on the distribution pattern by which Fe^{2+} is introduced into the Fe^{3+} matrix (i.e., with or without nearest-neighbor restrictions) and on the distribution of diamagnetic ions in the structure.

A computer method was developed to simulate the Fe^{2+} vs. intensity relationship. In the simulation model, the intensity was represented by the number of Fe^{2+}–O–Fe^{3+} moieties and the dioctahedral sheet consisted

https://doi.org/10.1346/CCMN.1987.0350507 Published online by Cambridge University Press

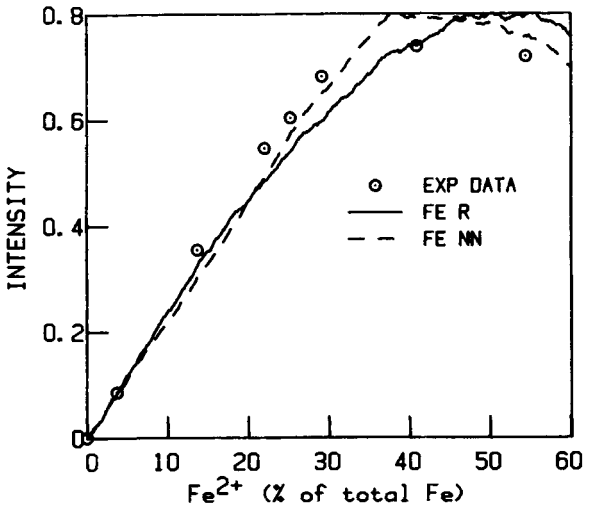

Figure 4. Comparison of observed intensity of the intervalence electron transfer band (O) relative to the unaltered nontronite SWa-1 with the intensity predicted by computer simulations with random (——) and nearest neighbor restricted (-----) distribution patterns for Fe^{2+}. Determination coefficients (r^2) were .96 and .99, respectively.

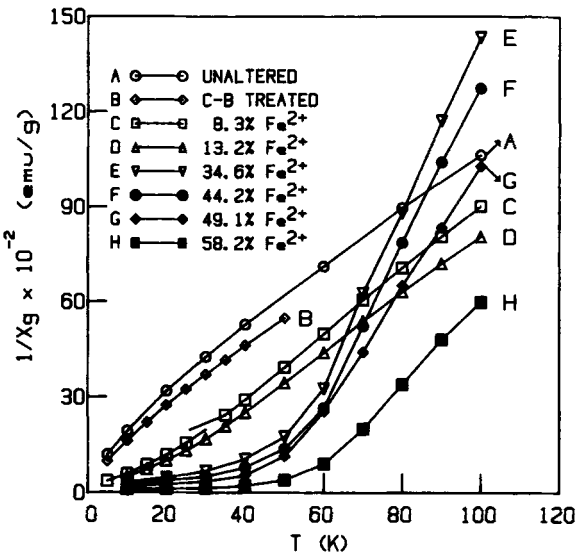

Figure 5. $1/\chi$ vs. T for reduced and unaltered SWa-1 powder samples obtained at 0.1 tesla. Curie-Weiss Law parameters, obtained from the linear portion of the curves, are listed in Table 2.

of 1600 cations distributed centrosymmetrically, i.e., 1200 Fe^{3+} ions and 400 diamagnetic (e.g., Al^{3+}, Mg^{2+} represented by Al) ions. Distribution schemes for the Al ions were either random or homogeneous. A random distribution pattern was used for the conversion of Fe^{3+} to Fe^{2+} during the reduction simulation, with either no restrictions (denoted R), or a nearest-neighbor restriction (denoted NN) which precluded Fe^{2+}–O–Fe^{2+} linkages until no other combinations were possible.

The data in Figure 3 suggest that the diamagnetic ion distribution (homogeneous or random) had little influence on the Fe^{2+}–O–Fe^{3+} vs. Fe^{2+} relationship. A marked difference, however, was noted between the two Fe^{3+}-reduction patterns. With no restrictions (R), the number of Fe^{2+}–O–Fe^{3+} linkages followed Fe^{2+} nonlinearly, whereas simulation with the nearest-neighbor restriction (NN) was close to linear until a critical value was reached (about 35–37% of the total Fe), beyond which the restriction could no longer be enforced. A comparison of these line shapes with the actual measured intensities (Figure 4) indicates that the NN model more closely matched the experimental results than the R model. The critical value in the model is less than 50% of the total Fe because of the presence of diamagnetic ions. A typical average environment around Fe^{2+} likely includes one Al and two Fe^{3+} ions at the critical value.

Magnetic exchange interactions

Based on the inverse susceptibility plots ($1/\chi$ vs. T) (Figure 5), samples can be divided naturally into four groups: A and B, C and D, E and F, and G and H, which correspond to degrees of reduction of 0%, 8–14%, 34–44%, and 49–58% of total Fe, respectively. All plots were analyzed using the Curie-Weiss law, $1/\chi = (T - \theta)/C$, in which χ is the measured susceptibility, C is the Curie constant, and θ is the Curie-Weiss paramagnetic temperature. The values of C and θ (Table 2) were obtained from the slope and x-intercept ($1/\chi = 0$), respectively, of the linear extrapolation of $1/\chi$ vs. T.

The first group consists of the unaltered (A) and C-B treated (B) SWa-1 samples. The value of $\theta = -19$ K for the unaltered sample is comparable to those reported previously of -20 K (Bonnin, 1981) and -27 K (Ballet and Coey, 1982). The negative value indicates that Fe^{3+}–O–Fe^{3+} exchange is antiferromagnetic. Plots of magnetization (M) vs. magnetic field (H) at 5 K for sample (A) are also characteristic of antiferromagnetic exchange (Figure 6). The failure of $1/\chi$ to increase sharply at low T (Figure 5) indicates that long-range magnetic ordering is absent, suggesting either chemical disorder or "frustration." The presence and distribution of diamagnetic cations could produce chemical disorder in the octahedral sheet by separating the magnetic cations into small, isolated clusters, thus preventing long-range ordering. Alternatively, "frustration" would occur if the immediate Fe neighbors of another Fe atom were neighbors of each other, thus precluding simultaneous satisfaction of all antiferromagnetic exchange, i.e., if two adjacent moments were aligned anti-parallel ($\uparrow\downarrow$), the third could not align anti-parallel to both. Hence, the system would be "frus-

https://doi.org/10.1346/CCMN.1987.0350507 Published online by Cambridge University Press

Table 2. Curie constants (C) and Curie-Weiss temperature (θ) determined for reduced and unaltered nontronite samples.

Fe^{2+} (% of total Fe)	C (emu/mole·K)	θ (K)
0	9.11	−19.2
8.3	8.02	11.0
13.2	8.92	12.3
34.6	2.97	47.8
44.2	3.22	49.3
49.1	4.22	46.9
58.2	6.31	53.6

trated." Similar conclusions can be drawn for the C-B treated sample. The effects of chemical disorder and frustration on long-range magnetic ordering in nontronites will be discussed in more detail by Lear and Stucki in a forthcoming publication.

A possible alternative explanation for the magnetic behavior of samples A and B is superparamagnetism. Superparamagnetic behavior at such low temperatures, however, is unlikely because of the large particle size of the clay mineral relative to known superparamagnetic minerals, such as ferrihydrite (Coey and Readman, 1973).

The other three groups (C and D, E and F, and G and H) in Figure 5 are comprised of reduced samples. As Fe^{3+} in the octahedral sheet is converted to Fe^{2+}, Fe^{2+}–O–Fe^{3+} pairs form to produce ferromagnetic interactions which lead to positive paramagnetic Curie temperatures of about 10 to 55 K, depending on the extent of reduction (Figure 5; Table 2). The magnetization curve for a reduced (Fe^{2+} = 22% of the total Fe) sample at 5 K (Figure 6) also indicates the presence of ferromagnetic interactions, showing the rapid saturation which is characteristic of a ferromagnet.

Samples C and D are slightly reduced and contain small amounts of Fe^{2+} in a Fe^{3+} structure, resulting in small domains of Fe^{2+}–O–Fe^{3+}. The susceptibility is dominated by the frustrated antiferromagnetic component seen in A and B, but the ferromagnetic component is sufficiently prominent to produce positive Curie-Weiss temperatures (Table 2). The moderately reduced samples (E and F) are dominated by ferromagnetic exchange in Fe^{2+}–O–Fe^{3+}. The amount of Fe^{2+} is sufficient (about 30–45% of the total Fe) that only a few unreduced domains remain in the structure. Finally, samples G and H have sufficiently large Fe^{2+} contents that Fe^{2+}–O–Fe^{2+} linkages form at the expense of Fe^{2+}–O–Fe^{3+}. The Fe^{2+}–O–Fe^{2+} linkages introduce an additional ferromagnetic component. The NN model for the distribution of Fe^{2+} dictates that these linkages occur only in highly reduced samples (Fe^{2+} >35% of the total Fe).

As stated above, ideally Fe^{3+}–O–Fe^{3+} linkages exhibit antiferromagnetic exchange; i.e., at the magnetic ordering temperature the lowest energy state is that in

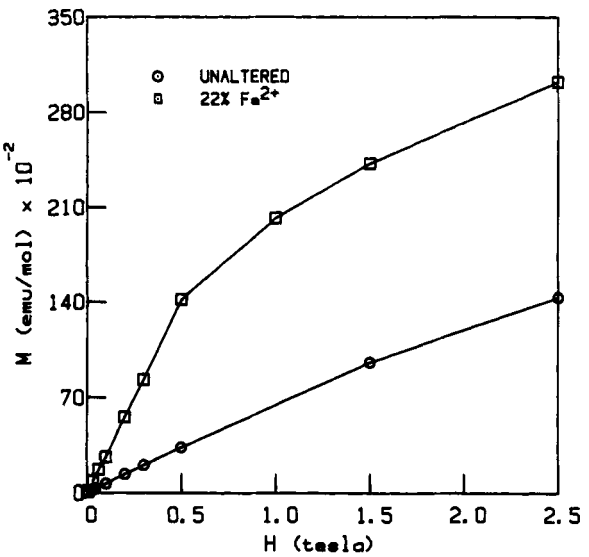

Figure 6. Magnetization curves at 5 K for reduced (Fe^{2+} = 22% of total Fe) and unaltered SWa-1 samples.

which the atomic magnetic moments on adjacent Fe atoms are aligned antiparallel. If a single Fe atom becomes reduced, however, the lowest energy state for magnetic ordering is that in which the non-exchanged electrons are aligned parallel, leading to ferromagnetic exchange. The inclusion of the extra electron due to reduction, therefore, causes a rearrangement in the relative positions of the energy levels for Fe–O–Fe linkages. This observed ferromagnetic exchange in the reduced sample suggests that the double exchange mechanism (Zener, 1951) may occur if Fe^{2+}–O–Fe^{3+} exchange takes place. This exchange involves the transfer of one electron, without changing spin, from Fe^{2+} to the shared O^{2-} ion and the simultaneous transfer of an electron with parallel spin from O^{2-} to Fe^{3+} (Figure 7). This double exchange can occur only if the non-exchanged electrons on the Fe atoms are aligned parallel, otherwise the exchange would violate the Pauli exclusion principle (i.e., any pair of electrons in an orbital must be aligned antiparallel) and thus be forbidden. Therefore, Zener's mechanism of double-exchange favors parallel alignment of spins of adjacent cations, leading to ferromagnetic exchange.

SUMMARY AND CONCLUSIONS

The reduction of structural Fe^{3+} in nontronite SWa-1 suggests a model in which Fe^{2+} is randomly distributed in a centrosymmetric Fe^{3+} matrix, with the restriction that no Fe^{2+}–O–Fe^{2+} pairs form until all possible Fe^{3+}–O–Fe^{2+} combinations have been made. Visible absorption spectra indicate that the prominent IT band at about 730 nm arises from electron charge transfer via vibronic coupling of Fe^{3+} and Fe^{2+} in adjacent octahedral sites, bridged through an O^{2-} ligand. Magnetic

https://doi.org/10.1346/CCMN.1987.0350507 Published online by Cambridge University Press

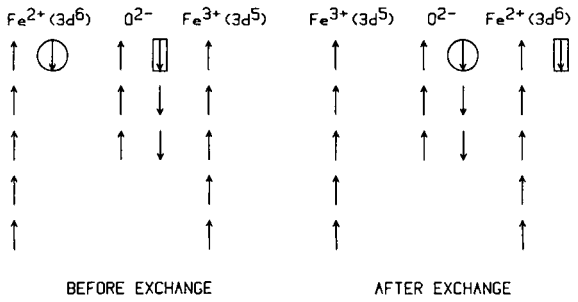

Figure 7. Proposed mechanism to account for the ferromagnetic coupling for a mixed-valence system (Zener, 1951). Exchanged electrons are indicated by enclosure in either a circle or rectangle.

exchange between Fe^{3+} ions were antiferromagnetic, but the presence of chemical disorder or frustration inhibited long-range ordering. The introduction of Fe^{2+} by chemical reduction produced a ferromagnetic component due to Fe^{2+}–O–Fe^{3+}. An additional ferromagnetic component, due to Fe^{2+}–O–Fe^{2+} interactions, was seen at higher levels of reduction (Fe^{2+} >35% of the total Fe).

ACKNOWLEDGMENTS

The authors gratefully acknowledge financial support of this project by the U.S. Army Research Office (Contract No. DAAG29-84-k-0167), and the Illinois Agricultural Experiment Station.

REFERENCES

Anderson, P. W. (1950) Antiferromagnetism. The theory of superexchange interaction: *Phys. Rev.* **79,** 350–356.

Anderson, P. W. (1959) New approach to the theory of superexchange interaction: *Phys. Rev.* **115,** 2–13.

Anderson, W. L. and Stucki, J. W. (1979) Effect of structural Fe^{2+} on visible absorption spectra of nontronite suspensions: in *Proc. Int. Clay Conf., Oxford, 1978,* M. M. Mortland and V. C. Farmer, eds., Elsevier, Amsterdam, 75–83.

Ballet, O. and Coey, J. M. D. (1982) Magnetic properties of sheet silicates; 2:1 layer minerals: *Phys. Chem. Miner.* **8,** 218–229.

Bonnin, D. (1981) Propriétés magnétiques liées aux désordres bidimensionnels dans un silicate lamellaire ferrique: La nontronite: These d'Etat, Université de Paris, 82 pp.

Bonnin, D., Calas, G., Suquet, H., and Pezerat, H. (1985) Sites occupancy of Fe^{3+} in Garfield nontronite: A spectroscopic study: *Phys. Chem. Minerals* **12,** 55–64.

Coey, J. M. D. and Readman, P. W. (1973) Characterisation and magnetic properties of natural ferric gel: *Earth Planet. Sci. Letters* **21,** 45–51.

Goodenough, J. B. (1963) *Magnetism and the Chemical Bond:* Interscience, New York, 393 pp.

Goodman, B. A., Russell, J. D., Fraser, A. R., and Woodhams, F. W. D. (1976) A Mössbauer and I.R. spectroscopic study of the structure of nontronite: *Clays & Clay Minerals* **24,** 53–59.

Hush, N. S. (1967) Intervalence transfer absorption. Part 2. Theoretical considerations and spectroscopic data: in *Progress in Inorganic Chemistry,* F. A. Cotton, ed., Interscience, New York, 357–390.

Kramers, H. A. (1934) L'interaction entre les atomes magnétogènes dans un cristal paramagnétique: *Physica* **1,** 182–192.

Lear, P. R. and Stucki, J. W. (1985) Role of structural hydrogen in the reduction and reoxidation of iron in nontronite: *Clays & Clay Minerals* **33,** 539–545.

Schatz, P. N. (1980) A vibronic coupling model for mixed-valence compounds and its application to real systems: in *Mixed-Valence Compounds,* D. B. Brown, ed., D. Reidel, Boston, 115–188.

Stucki, J. W. (1981) The quantitative assay of minerals for Fe^{2+} and Fe^{3+} using 1,10-phenanthroline: II. A photochemical method: *Soil Sci. Soc. Amer. J.* **45,** 638–641.

Stucki, J. W. (1987) Structural iron in smectites: in *Iron in Soils and Clay Minerals,* J. W. Stucki, B. A. Goodman, and U. Schwertmann, eds., D. Reidel, Dordrecht, 625–675.

Stucki, J. W., Golden, D. C., and Roth, C. B. (1984) Effects of reduction and reoxidation of structural iron on the surface charge and the dissolution of dioctahedral smectites: *Clays & Clay Minerals* **32,** 350–356.

Zener, C. (1951) Interaction between the *d* shells in the transition metals: *Phys. Rev.* **81,** 440–444.

(Received 2 February 1987; accepted 24 March 1987; Ms. 1639)